



# Fabrication and mechanical properties of in situ TiC/Ti metal matrix composites

Liu Yanbin<sup>a</sup>, Liu Yong<sup>a,\*</sup>, Tang Huiping<sup>b</sup>, Wang Bin<sup>a</sup>, Liu Bin<sup>a</sup>

<sup>a</sup> State Key Lab of Powder Metallurgy, Central South University, Changsha 410083, Hunan, PR China

<sup>b</sup> State Key Laboratory of Porous Metals, Northwestern Research Institute of Nonferrous Metals, Xi'an 710012, PR China

## ARTICLE INFO

### Article history:

Received 18 July 2010

Received in revised form

29 November 2010

Accepted 13 December 2010

Available online 22 December 2010

### Keywords:

Metal matrix composites

Powder metallurgy

Hot rolling

## ABSTRACT

In situ TiC particle reinforced titanium matrix composites (TMCs) were successfully fabricated by reactive sintering of Ti + Mo<sub>2</sub>C and Ti + VC compacts. The results of the tensile tests at ambient and elevated temperatures show that the strength of the composites increases with increasing additive content (Mo<sub>2</sub>C and VC), and decreases with increasing temperatures. Comparing the two types of TMCs, the Ti + VC composites have a lower strength than the Ti + Mo<sub>2</sub>C composites, but can more effectively retain the strength to elevated temperatures. Microstructural analyses show that the main strengthening mechanisms of the TMCs are solid solution, grain refinement and particulate strengthening. Different dominant strengthening mechanisms in different composites are responsible for the variations of the mechanical properties. At elevated temperatures, the volume fraction of TiC particles is the main factor for increasing the strength.

© 2010 Elsevier B.V. All rights reserved.

## 1. Introduction

The interest in discontinuously reinforced titanium matrix composites (TMCs) has increased in recent years due to the low cost, easy fabrication and excellent mechanical properties [1–4]. Several ceramic particles were proposed as reinforcements [1–7]: SiC, TiN, TiC and TiB. Of these TiB and TiC are the most frequently used [1–4,7]. The mechanical properties of TMCs have been found to be mainly dependent upon the composition and the microstructure of both the matrix and the particles. However, the most important way to ensure the strength and the stiffness of the composites is to control the interface. Inadequate bonding between the metallic matrix and the ceramic reinforcement may lead to poor mechanical properties of metal-matrix composites. The in situ synthesis is an effective method to enhance the bonding between particle and matrix by formation of a clean interface. Recently several processing techniques for synthesizing the in situ ceramic reinforcements have been developed, including reactive sintering [2,3,8], mechanical alloying [9], casting [10] and gas–solid reaction [11]. The reactive sintering process seems to be a promising way to fabricate TMCs due to its low-cost and simplicity. In situ ceramics reinforced TMCs fabricated by reactive sintering are formed through the exothermic reaction between the additives and the Ti matrix. Many reactive systems [2,3,6,8–11]: Ti–TiB<sub>2</sub>, Ti–B, Ti–B<sub>4</sub>C, Ti–BN, Ti–ReB<sub>6</sub>, Ti–MB are used to fabricate in situ ceramic reinforcements. The reactive sinter-

ing of titanium and metal carbides such as VC, Mo<sub>2</sub>C, Cr<sub>2</sub>C<sub>3</sub> not only provides the carbon to form TiC particles but also introduces solutes of Mo, V and Cr in the Ti matrix [3,12,13]. Hence, the addition of metal carbides may improve the mechanical properties of the TMCs very effectively. An understanding of the mechanical behaviors of the composites is essential to optimize the process.

This paper aims to investigate: (1) microstructure evolution during the fabrication of in situ TiC reinforced TMCs using reactive sintering and post thermomechanical treatment, and (2) the mechanical behaviors of the composites at ambient temperature and elevated temperatures.

## 2. Experimental

The composition of the TMCs is listed in Table 1. The raw powders were blended in a high-efficiency blender for 1 h under an Ar atmosphere. Ti powder (<104 μm) and Mo<sub>2</sub>C (<2 μm) or VC (<2 μm) powder were blended. The mixed powders were cold isostatically pressed to round bars with a diameter of 45 mm at a pressure of 400 MPa. Then the powder compacts were sintered at 1300 °C for 1.5 h in a vacuum of  $5 \times 10^{-3}$  Pa, followed by furnace cooling. In order to achieve fully densified materials, the as-sintered TMCs were hot rolled to 10 mm rods after heating to a temperature of 1000 °C with a rolling ratio of about 20. The strength and the ductility of the hot rolled TMCs after annealing at 650 °C for 2 h were tested. The tensile tests were carried out on a CSS-4400 test machine using smooth specimens with a gauge size of d5 mm × 25 mm at a constant cross head speed of 2 mm/min. Each value is an average of three measurements. Specimens for microstructural investigation after hot rolling were sectioned parallel to the rolling axis. The microstructures of the composites were investigated using an optical microscope (OM) and a scanning electron microscope (SEM) in the backscattered mode (BSE). The phase transformation was studied by X-ray diffraction analysis (XRD). The average particle size in the each TMC was determined from a sample of at least 15 SEM micrographs.

\* Corresponding author. Tel.: +86 731 88830406; fax: +86 731 88710855.  
E-mail address: [yonliu1@yahoo.com.cn](mailto:yonliu1@yahoo.com.cn) (L. Yong).

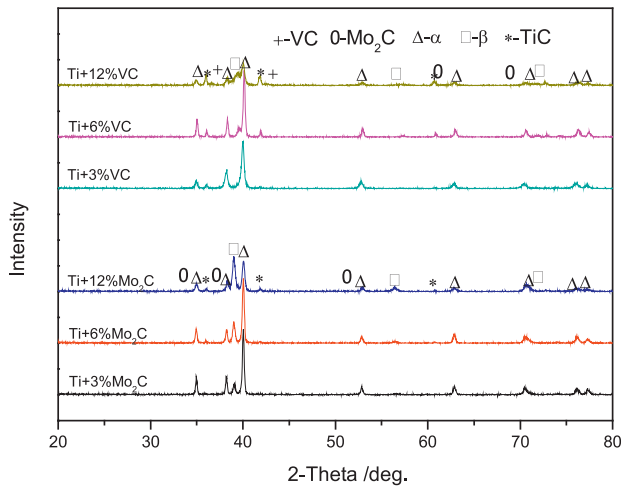


**Fig. 1.** XRD patterns of the as-sintered titanium matrix composites.

### 3. Results

#### 3.1. Microstructures

**Fig. 1** shows X-ray diffraction patterns of the as-sintered TMCs. It indicates that only three phases can be found in the present composites, which are  $\alpha$ -Ti,  $\beta$ -Ti and TiC. The results of the XRD analyses confirm the formation of TiC by reactive sintering of Ti + Mo<sub>2</sub>C and Ti + VC compacts. The microstructures of as-sintered TMCs are shown in **Fig. 2**. The TMCs with 3 wt.% and 6 wt.% additives show a typical  $\alpha$  +  $\beta$  colony structure with aligned  $\alpha$  platelets separated by thin  $\beta$  laths, and  $\alpha$  phases at the grain boundaries. The TMCs with 12 wt.% additives show a dominant  $\beta$ -phase microstructure. **Fig. 2** also shows the formation of TiC clusters in the Ti + Mo<sub>2</sub>C composites. However, the TiC particles are homogeneously distributed in the matrix of the Ti + VC composites. The Ti + 3%Mo<sub>2</sub>C composite has the smallest TiC particles size in all the composites, ranging from 3 to 5  $\mu$ m. While the TiC particles sizes in the other composites are ranging from 5 to 15  $\mu$ m.

The distribution of TiC particles in the TMCs after hot rolling is shown in **Fig. 3**. In the Ti + Mo<sub>2</sub>C composites, the clusters of TiC particles tend to align along the rolling direction. However, TiC particles in the Ti + VC composites distribute relatively uniform. Little

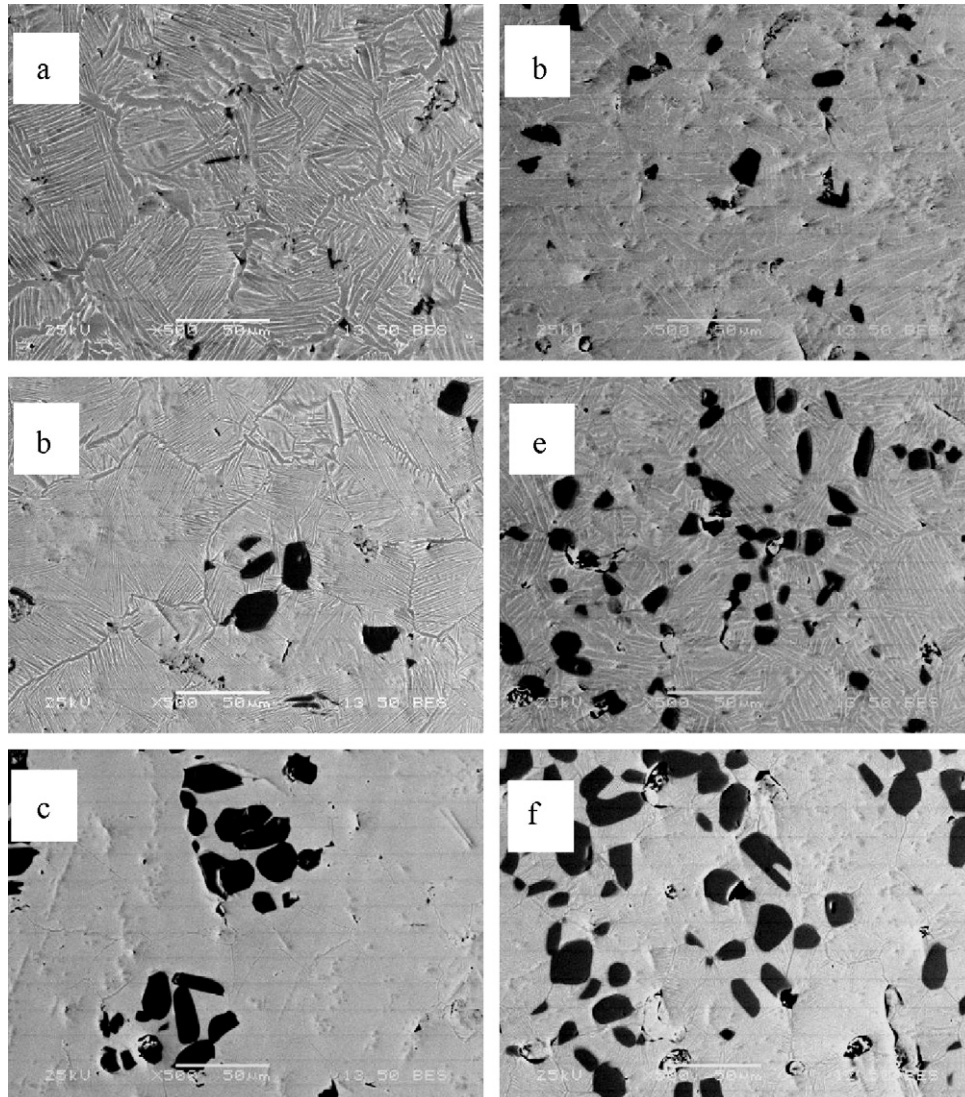


**Fig. 2.** Microstructures of the as-sintered titanium matrix composites: (a) Ti + 3%Mo<sub>2</sub>C; (b) Ti + 6%Mo<sub>2</sub>C; (c) Ti + 12%Mo<sub>2</sub>C; (d) Ti + 3%VC; (e) Ti + 6%VC; (f) Ti + 12%VC.

**Table 1**  
Weight percentage of raw materials and designed volume ratio of TiC in composites.

Composite	Ti + Mo <sub>2</sub> C			Ti + VC		
	Ti + 3%Mo <sub>2</sub> C	Ti + 6%Mo <sub>2</sub> C	Ti + 12%Mo <sub>2</sub> C	Ti + 3%VC	Ti + 6%VC	Ti + 12%VC
Metal carbide (wt.%)	3	6	12	3	6	12
Metal carbide (vol.%)	1.4	3	6.3	2.3	4.7	9.6
Metal elemental (wt.%)	2.82	5.64	11.28	2.48	4.96	9.92
Carbon elemental (wt.%)	0.18	0.36	0.72	0.52	1.04	2.08
Designed TiC (vol.%)	0.7	1.4	2.8	2.1	4.2	8.4

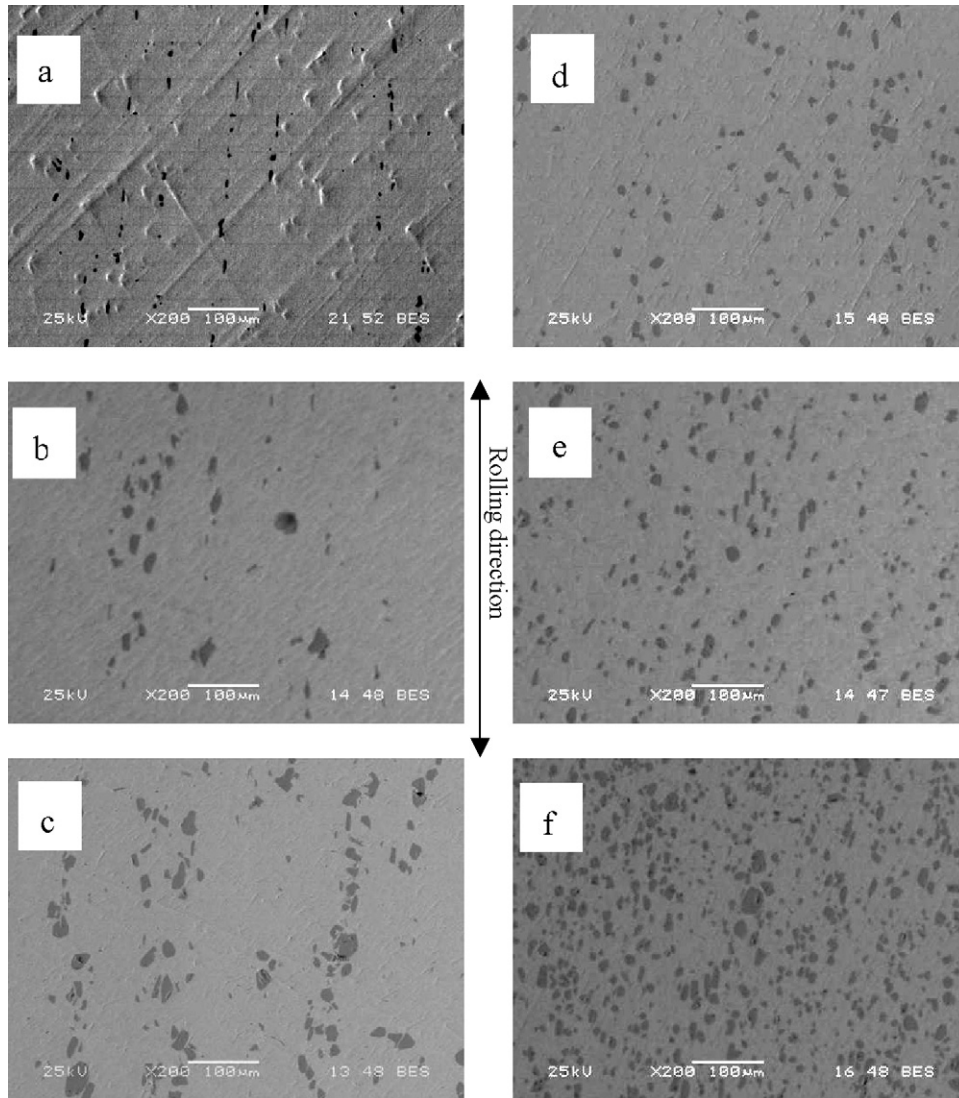


**Fig. 3.** The distributions of TiC particles of the hot rolled titanium matrix composites: (a) Ti + 3%Mo<sub>2</sub>C; (b) Ti + 6%Mo<sub>2</sub>C; (c) Ti + 12%Mo<sub>2</sub>C; (d) Ti + 3%VC; (e) Ti + 6%VC; (f) Ti + 12%VC.

**Table 2**  
Average TiC particle size (μm) of the composites.

Composite	Ti + Mo <sub>2</sub> C			Ti + VC		
	Ti + 3%Mo <sub>2</sub> C	Ti + 6%Mo <sub>2</sub> C	Ti + 12%Mo <sub>2</sub> C	Ti + 3%VC	Ti + 6%VC	Ti + 12%VC
Sintering condition	4.6	10.9	12.7	11.5	11.7	13.4
Hot rolling condition	5.1	11.8	13.2	10.2	12.2	13.9

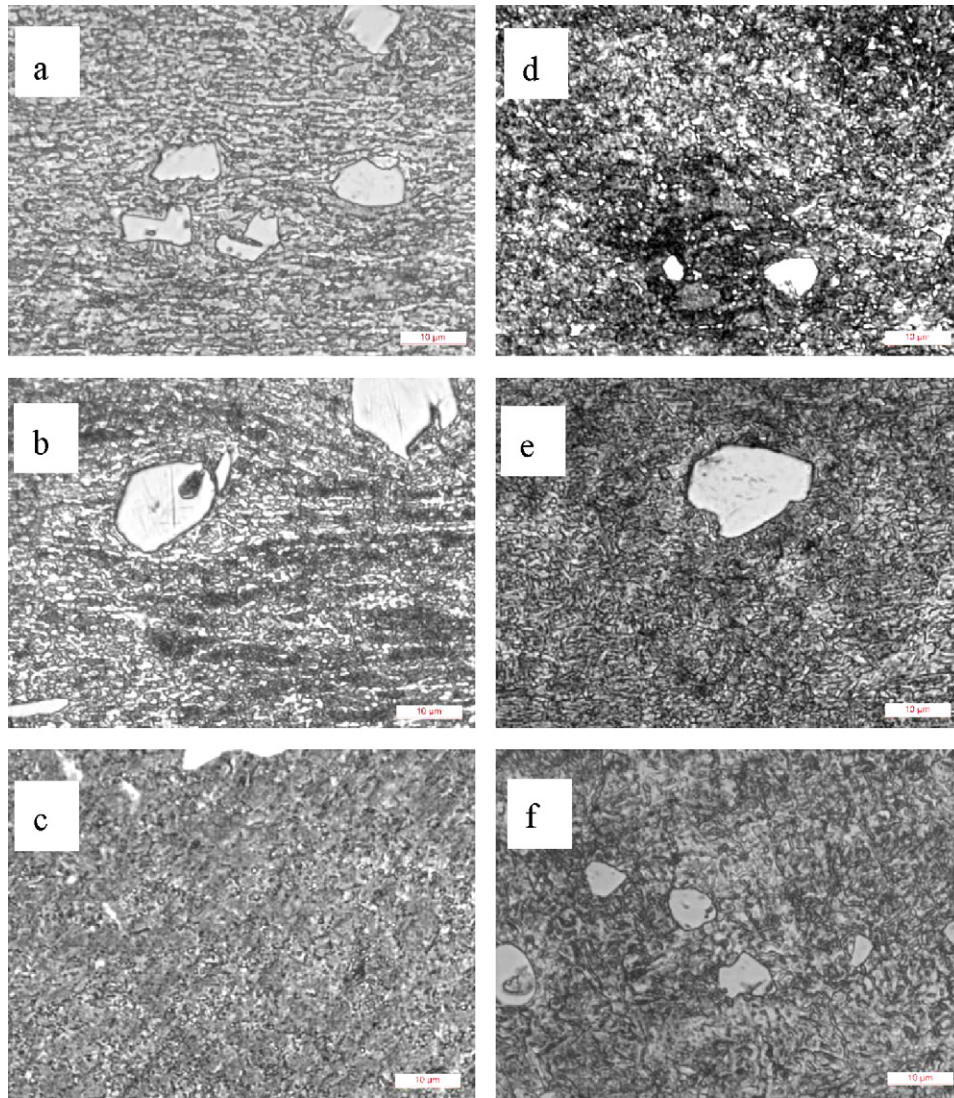


**Fig. 4.** Optical microstructures of the thermal-mechanically treated titanium matrix composites: (a) Ti + 3%Mo<sub>2</sub>C; (b) Ti + 6%Mo<sub>2</sub>C; (c) Ti + 12%Mo<sub>2</sub>C; (d) Ti + 3%VC; (e) Ti + 6%VC; (f) Ti + 12%VC.

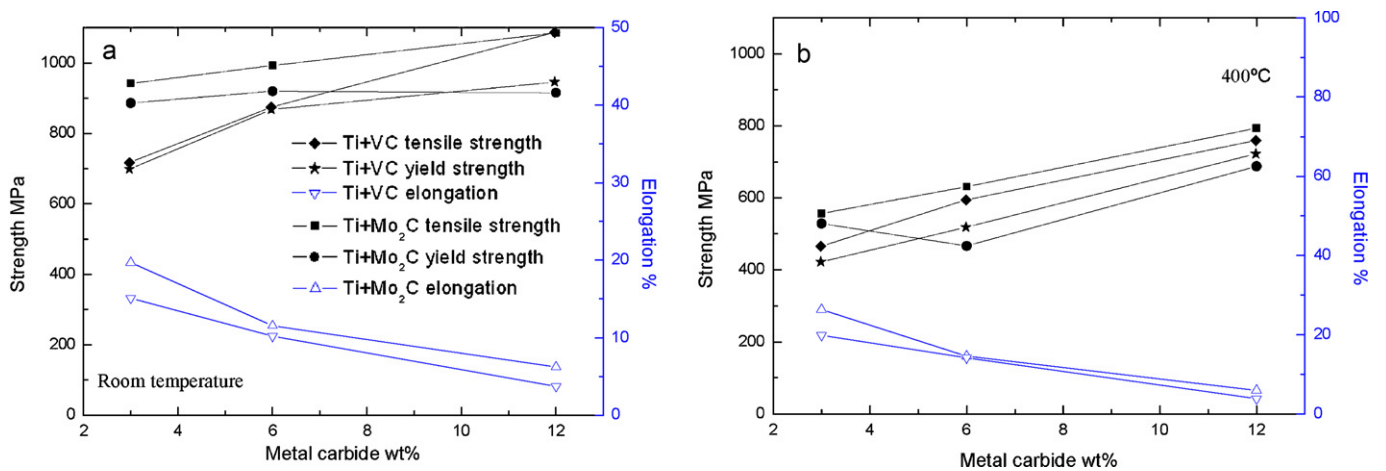


**Fig. 5.** The tensile properties of the composites after hot rolling and annealing at 650 °C/2 h tested at: (a) ambient temperature; (b) 400 °C; (c) 500 °C; (d) 600 °C.

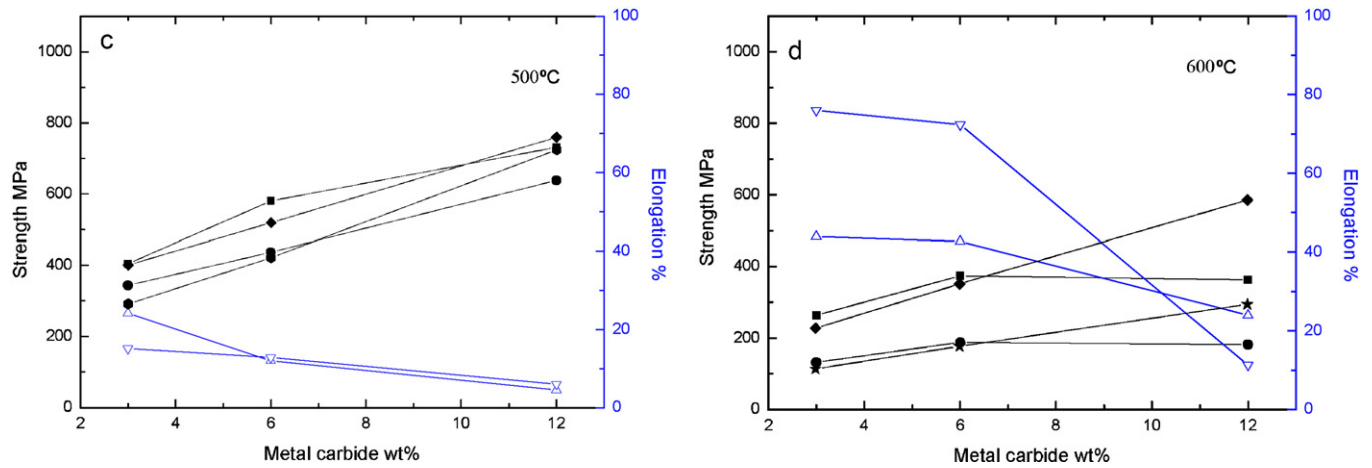


Fig. 5. (Continued).

change in the TiC particle size can be found in the TMCs after the hot rolling (see the average TiC particle size in Table 2). By etching, the microstructures of the titanium matrices after hot rolling and annealing can be clearly seen, as shown in Fig. 4. Significant grain refinement occurs during the thermal mechanical treatment and a grain size as small as 1  $\mu\text{m}$  can be obtained.

### 3.2. Mechanical properties at ambient and elevated temperatures

The mechanical properties of the TMCs after hot rolling and annealing at 650  $^{\circ}\text{C}$  for 2 h at ambient and elevated temperatures are shown in Fig. 5. The ultimate tensile and yield strength of the Ti + Mo<sub>2</sub>C and Ti + VC composites at ambient temperature increase

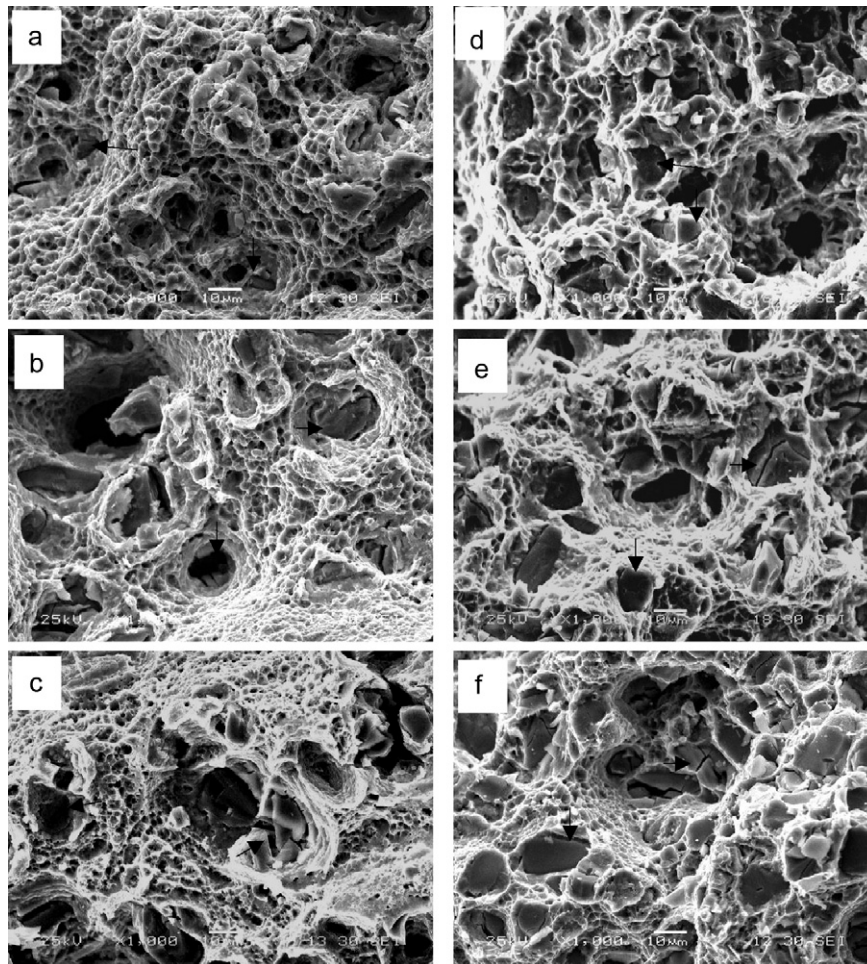
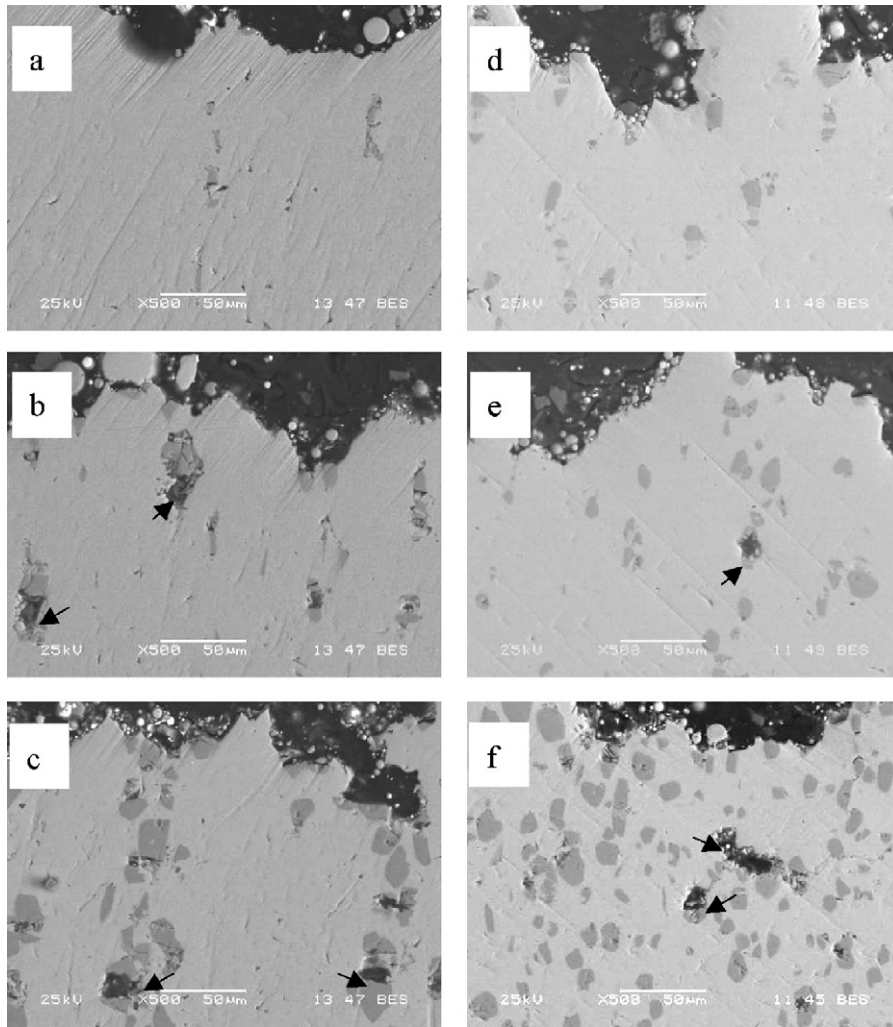
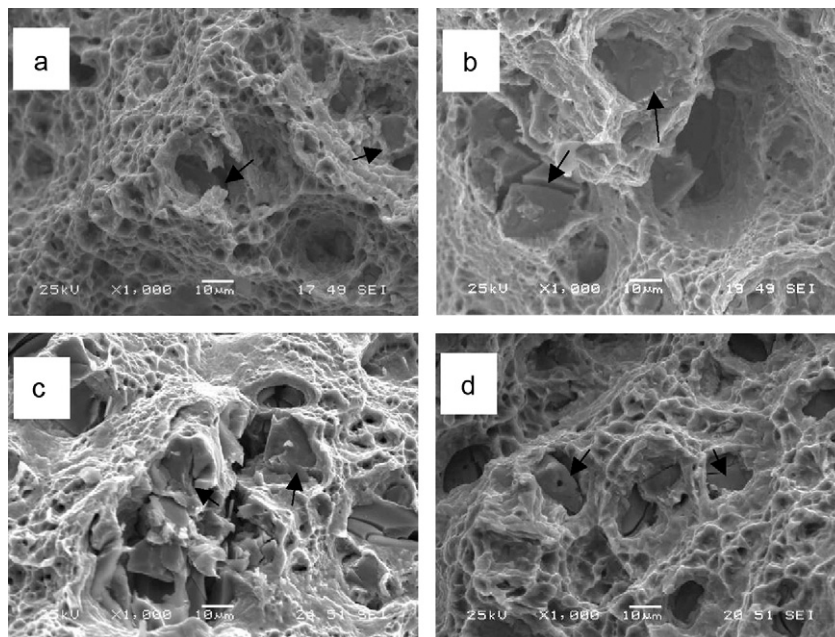


Fig. 6. Scanning electron micrographs of tensile fracture surface of the titanium matrix composites tested at ambient temperature: (a) Ti + 3%Mo<sub>2</sub>C; (b) Ti + 6%Mo<sub>2</sub>C; (c) Ti + 12%Mo<sub>2</sub>C; (d) Ti + 3%VC; (e) Ti + 6%VC; (f) Ti + 12%VC; the cracked TiC particles are marked by arrows.



**Fig. 7.** SEM micrographs of cross-sections of titanium matrix composites near the fracture surfaces: (a) Ti+3%Mo<sub>2</sub>C; (b) Ti+6%Mo<sub>2</sub>C; (c) Ti+12%Mo<sub>2</sub>C; (d) Ti+3%VC; (e) Ti+6%VC; (f) Ti+12%VC; the micro-voids are marked by arrows.



**Fig. 8.** Scanning electron micrographs of tensile fracture surface of the composites tested at temperatures of 400 °C: (a) Ti+3%Mo<sub>2</sub>C; (b) Ti+6%Mo<sub>2</sub>C; (c) Ti+12%Mo<sub>2</sub>C; (d) Ti+3%VC; (e) Ti+6%VC; (f) Ti+12%VC; the cracked TiC particles are marked by arrows.

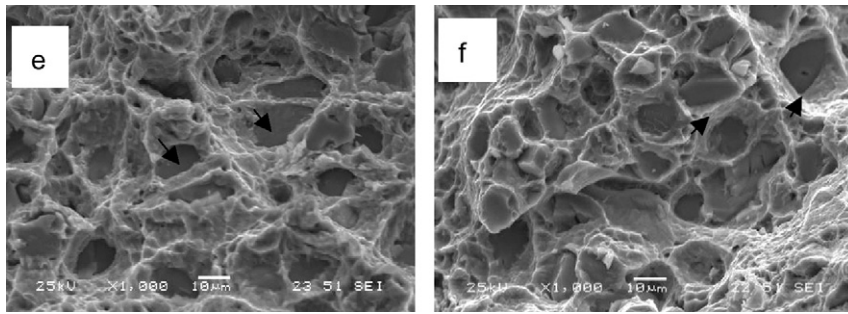


Fig. 8. (Continued).

linearly with the increase of additives ( $\text{Mo}_2\text{C}$  and VC). Comparing the two types of TMCs, the tensile strength and the ductility of the Ti +  $\text{Mo}_2\text{C}$  composites appear to be higher than the Ti + VC composites at the same contents of additives. The Ti +  $\text{Mo}_2\text{C}$  composites show a slower strength increment than the Ti + VC composites, and the difference in strength between the two types of the TMCs decrease with increasing additive. The increment of strength by the addition of  $\text{Mo}_2\text{C}$  in titanium is about 17.8 MPa per weight percent, and is much lower than 50 MPa per weight percent of pure Mo in titanium as reported in Ref. [14]. However, the increment of strength by the addition of VC in titanium is about 29.3 MPa per weight percent, and is very close to 35 MPa per weight percent of pure V addition as reported in Ref. [14]. The ductility of the TMCs

decreases with increasing additive. The ultimate tensile and yield strength of the Ti +  $\text{Mo}_2\text{C}$  and Ti + VC composites at temperatures of 400, 500 and 600 °C also linearly increase with increasing additive. The tensile strength of the Ti +  $\text{Mo}_2\text{C}$  composites is also higher than that of the Ti + VC composites as already observed at ambient temperature. The difference in strength between the two types of composites is reduced with the increase of the test temperatures and the additive content.

### 3.3. Fractography

The fracture surfaces of the TMCs at ambient temperature are shown in Fig. 6. It shows a brittle fracture manner in the TiC particles

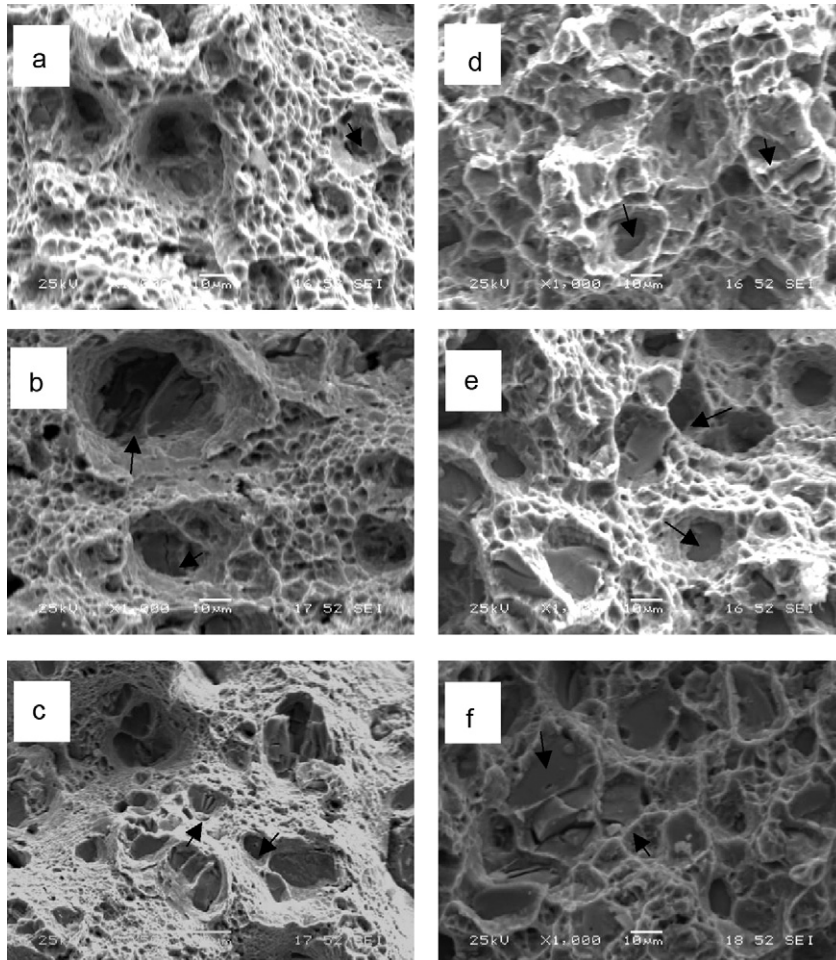
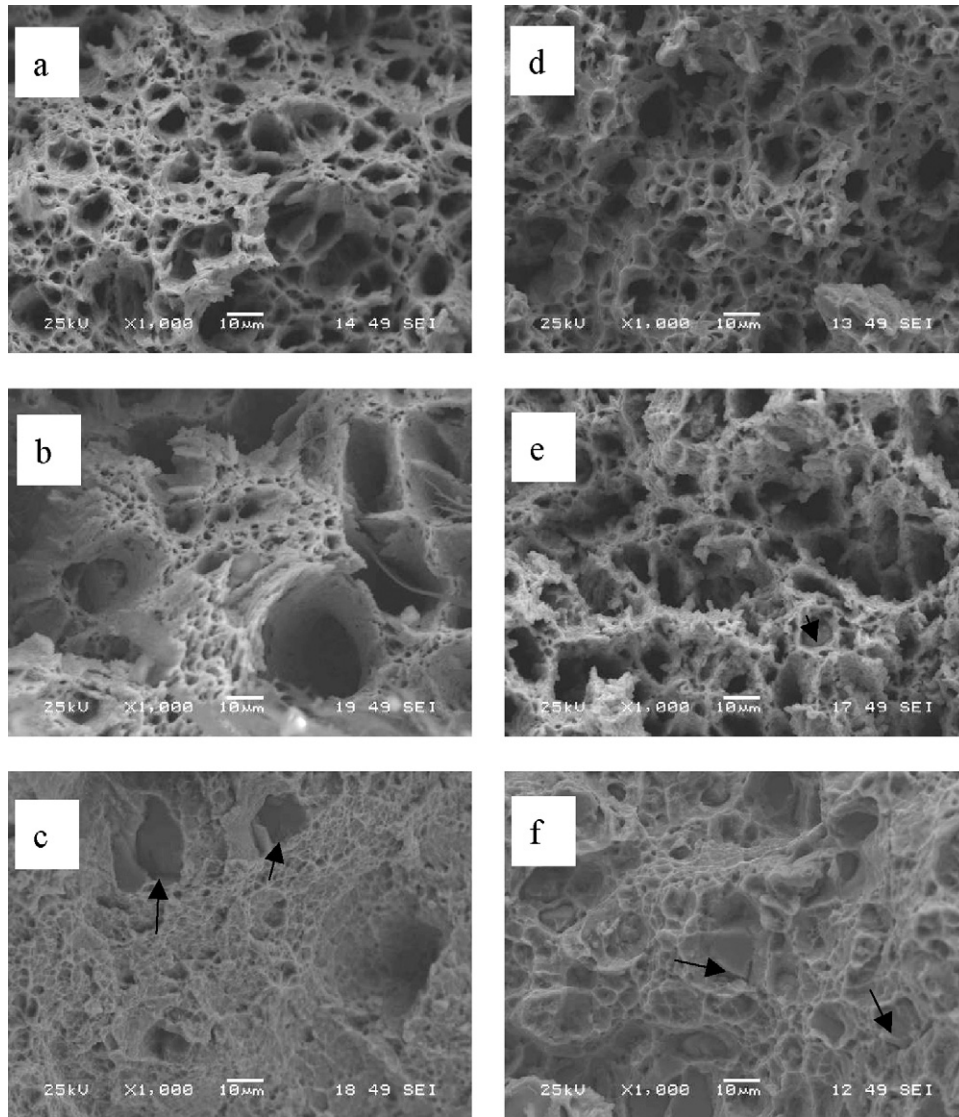


Fig. 9. Scanning electron micrographs of tensile fracture surface of the composites tested at temperature of 500 °C: (a) Ti + 3% $\text{Mo}_2\text{C}$ ; (b) Ti + 6% $\text{Mo}_2\text{C}$ ; (c) Ti + 12% $\text{Mo}_2\text{C}$ ; (d) Ti + 3%VC; (e) Ti + 6%VC; (f) Ti + 12%VC; the cracked TiC particles are marked by arrows.



**Fig. 10.** Scanning electron micrographs of tensile fracture surface of the composites tested at temperature of 600 °C: (a) Ti + 3%Mo<sub>2</sub>C; (b) Ti + 6%Mo<sub>2</sub>C; (c) Ti + 12%Mo<sub>2</sub>C; (d) Ti + 3%VC; (e) Ti + 6%VC; (f) Ti + 12%VC; the cracked TiC particles are marked by arrows.

and ductile manner in the matrix. The coalescence of micro-voids in the matrix as well as cleavages in the particles can be observed. As the content of the additives increases, the amount of fractured particles increases. Comparing the two types of TMCs, the fractured particles distribute more homogeneously in the Ti + VC composites than in the Ti + Mo<sub>2</sub>C composites. In order to understand the fracture process of the TMCs, the longitudinal sections of the fractured tensile specimens were examined, as shown in Fig. 7. The number of the micro-voids beneath the surface in the Ti + Mo<sub>2</sub>C composites increases with the increase of Mo<sub>2</sub>C content. However there are less micro-voids found in the Ti + VC composites. The fractographs of the TMCs at elevated temperatures (400, 500 and 600 °C) are shown in Figs. 8–10. The fracture characteristics of the TMCs at 400 °C are similar to that at ambient temperature, except for some large dimples due to the particle debonding. At 500 °C, more large dimples due to debonding can be detected, and this is more pronounced in the Ti + Mo<sub>2</sub>C composites than in the Ti + VC composites. There are no fractured TiC particles in the TMCs tested at a temperature of 600 °C, except for in the Ti + 6%VC and Ti + 12%VC composites. This indicates that the dominant fracture mechanism of the TMCs at high temperatures is particle debonding.

#### 4. Discussion

A number of strengthening mechanisms are operative in TMCs [14–18]. According to the results presented above, the mechanical strength of the TMCs prepared by addition of metal carbides in titanium mainly results from two aspects: solid solution and TiC particle formation. The strengthening effect due to the formation of solid solution is well described by Kolachev's empirical relation which can be applied to estimate the matrix strength of the TMCs [14,19]. Hence the strength increment due to the formation of TiC particles can be calculated by the following Eq. (1):

$$\Delta\sigma_{\text{TiC}} = \sigma_{\text{composite}} - \sigma_{\text{matrix}} \quad (1)$$

where  $\Delta\sigma_{\text{TiC}}$  is the strength increment due to the formation of TiC;  $\sigma_{\text{composite}}$  is the strength of the composite; and  $\sigma_{\text{matrix}}$  is the calculated strength of the matrix by Kolachev's empirical relation. The relationship between the increase of strength by TiC formation, composite strength and the matrix strength vs. the weight percent of metal carbides for different volume fractions of TiC particles are shown in Fig. 11. It is indicated that the strength increment by TiC hardening is not monotonously increased with its volume frac-



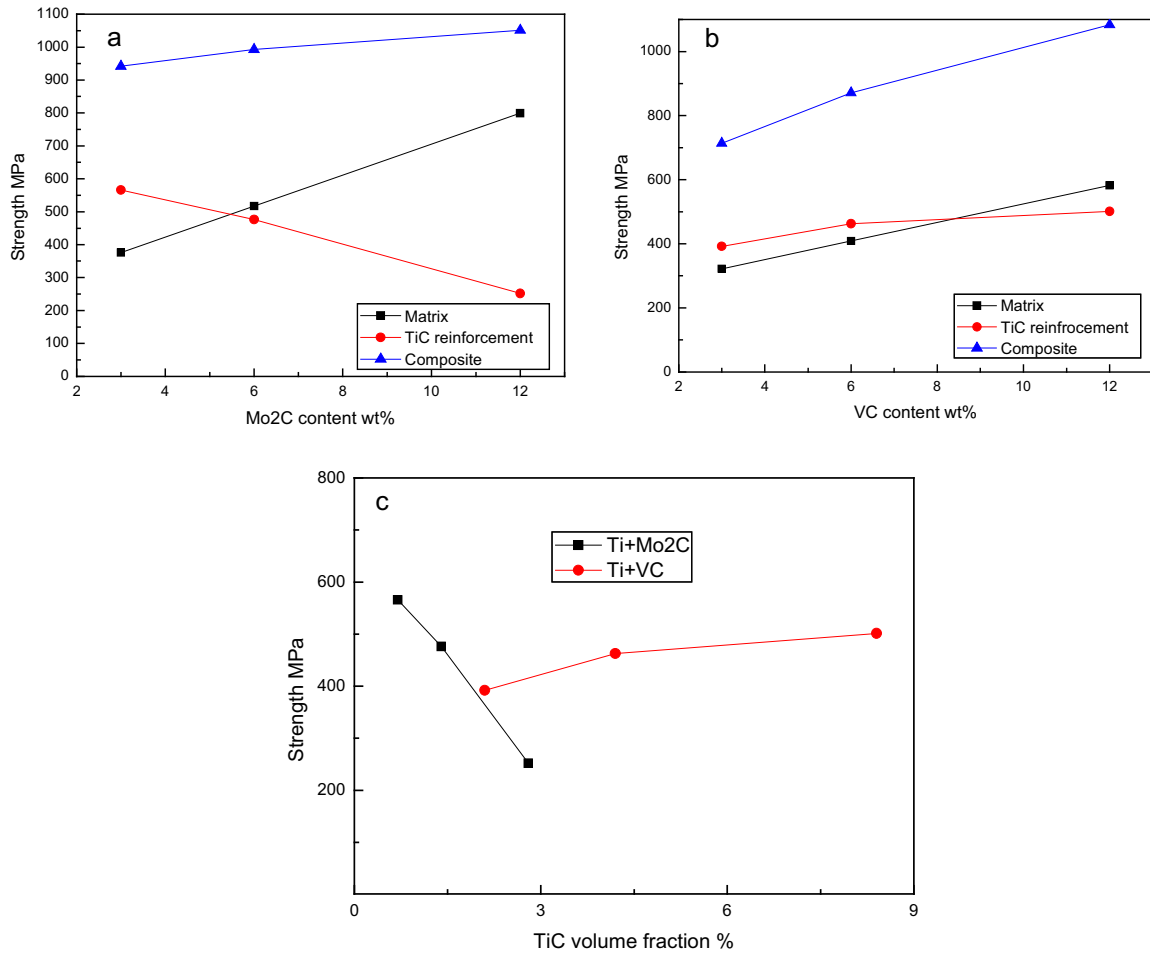


**Fig. 11.** The relationship between increased strength of TiC, composite strength and matrix strength vs. the weight percent of metal carbides: (a) Ti + Mo<sub>2</sub>C composites, (b) Ti + VC composites and (c) the increased strength changes with volume fraction of TiC particle.

tion, which on the contrary decreases in Ti + Mo<sub>2</sub>C composites and only slightly increases in Ti + VC composites. The formation of TiC particles contributes to the strengthening of the composite for two reasons. The first one is due to the grain refinement [3] enhanced by the TiC particles during the thermal mechanical processing (Fig. 4). But Fig. 4 also shows that the grain refinement effect of TiC is not linearly with its volume fraction. This may be attributed to the fact that the grain size has a certain equilibrium value for the fabrication process. Hence, the strengthening effect by grain refinement is similar for all of these materials. The second factor is the strengthening effect of TiC particles [15,16]. A number of studies have shown that the distribution of reinforcements greatly influences the deformation behaviors and mechanical properties of TMCs [20–23]. Wang et al. have speculated that triaxial stresses in the matrix are generally higher in clustered regions of four or more particles, thus shielding the centre of the cluster from plastic flow due to the higher local levels of constraint imposed on the matrix [23]. However, as shown in Fig. 7, damage forms preferentially in regions of TiC particle clustering during tensile deformation, and greatly decreases the strength of the Ti + Mo<sub>2</sub>C composites. Therefore, the strength increment caused by TiC-formation decreases in the Ti + Mo<sub>2</sub>C composites with the increase of its volume fraction. In the Ti + VC composites, the TiC particles are homogeneously distributed in the TMCs and a uniform deformation occurs (Fig. 7). According to the Nardone and Prewé model, the strengthening effect is proportional to the

volume fraction of TiC [24,25]. Hence, from the little change of the volume fraction of TiC results a slight increase in strength. For the Ti + Mo<sub>2</sub>C composites, the high strength is more due to the strong solid solution strengthening effect of Mo in titanium [14].

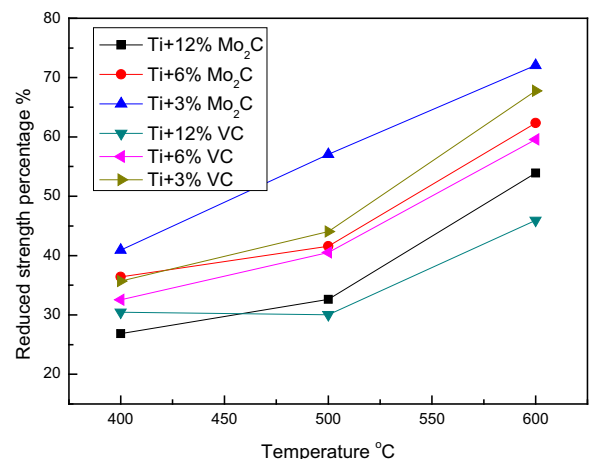


**Fig. 12.** The reduced strength percentages vs. the test temperatures.

The reduced strength at test temperatures are calculated as the following Eq. (2):

$$\sigma_{\text{reduced}} \% = \frac{\sigma_{\text{ambient temperature}} - \sigma_{\text{test temperature}}}{\sigma_{\text{ambient temperature}}} \times 100\% \quad (2)$$

where  $\sigma_{\text{reduced}}$  is the reduced strength at a test temperature;  $\sigma_{\text{ambient temperature}}$  is the tensile strength at ambient temperature; and  $\sigma_{\text{test temperature}}$  is the tensile strength at a test temperature. The reduced strength changes with test temperatures are plotted in Fig. 12. It can be clearly seen that the reduced strength decreases with the increase of content of the additives. And increases with increase of the test temperatures. The strengthening mechanisms at ambient temperature also work at elevated temperatures. However, the TiC particulate strengthening mechanism is less temperature dependent than the solid solution and grain refining strengthening mechanisms. It is suggested that the fractured other than pulled out reinforced particle in fracture surfaces of TMCs is the indication that the particulate strengthening takes place during deformation [26]. There are more cracked TiC particles in the fracture surfaces of the Ti + VC composites compared to the Ti + Mo<sub>2</sub>C composites (Figs. 8–10), also suggests the stronger strengthening effect caused by higher volume fraction of TiC particles. Therefore, the reduced strength of the Ti + Mo<sub>2</sub>C composites is higher than that of the Ti + VC composites at 500 and 600 °C due to a lower volume fraction of TiC particles. So, a high volume fraction of TiC particles contributes more in retaining the strength at elevated temperatures.

## 5. Conclusions

- (1) In situ TiC particles reinforced Ti(Mo) and Ti(V) titanium matrix composites are successfully fabricated by reactive sintering. The thermo mechanical treatment after sintering helps to refine the matrix microstructure and to homogenize the distribution of particles.
- (2) The strengthening increment due to formation of TiC particles is decreased with increase in the volume fraction of the Mo<sub>2</sub>C addition, while it is increased in Ti + VC composites. The inhomogeneous distribution of TiC particles is the main reason for this decrease in the strength in Ti + Mo<sub>2</sub>C composites.
- (3) At elevated temperatures, the volume percent of TiC particles is the major factor for the strengthening of TMCs.

## Acknowledgements

This work is supported by the Minister of Science & Technology of China under Contract No. 2007BAE07B05, the Graduate Degree Thesis Innovation Foundation of Central South University under the Grant No. 1960-71131100005, and the Innovative Fund of the State Key Lab of P/M.

## References

- [1] S. Gorsse, D.B. Miracle, *Acta Mater.* 51 (2003) 2427–2442.
- [2] J.Q. Lu, J.N. Qin, W.J. Lu, Y. Liu, J.J. Gu, D. Zhang, *J. Alloy Compd.* 469 (2009) 116–122.
- [3] Y. Liu, L.F. Chen, H.P. Tang, C.T. Liu, B. Liu, B.Y. Huang, *Mater. Sci. Eng. A* 418 (2006) 25–35.
- [4] D.R. Ni, L. Geng, J. Zhang, Z.Z. Zheng, *Mater. Sci. Eng. A* 478 (2008) 291–296.
- [5] C. Poletti, M. Balog, T. Schubert, V. Liedtke, C. Edtmaier, *Compos. Sci. Technol.* 68 (2008) 2171–2177.
- [6] Z.Y. Ma, S.C. Tjong, *L. Gen, Scripta Mater.* 42 (2000) 367–373.
- [7] D.G. Konitzer, M.H. Loretto, *Acta Mater.* 37 (1989) 397–406.
- [8] B.V.R. Bhat, J. Subramanyam, V.V.B. Prasad, *Mater. Sci. Eng. A* 325 (2002) 126–130.
- [9] A. Vyas, K.P. Rao, Y.V.R.K. Prasad, *J. Alloy Compd.* 475 (2009) 252–260.
- [10] W.J. e Lu, D. Zhang, X.N. Zhang, R.J. Wu, *Scripta Mater.* 44 (2001) 2449–2455.
- [11] Y.J. Kim, H. Chung, S.J.L. Kang, *Composites A* 32 (2001) 731–738.
- [12] B. Liu, Y. Liu, X.Y. He, H.P. Tang, L.F. Chen, B.Y. Huang, *Metall. Mater. Trans. A* 38 (2007) 2825–2831.
- [13] M. Hagiwara, N. Arimoto, S. Emura, Y. Kawabe, H.G. Suzuk, *ISIJ Int.* 32 (1992) 909–916.
- [14] V.N. Mosieyev, *Titanium Alloys Russian Aircraft and Aerospace Applications*, CRC Press, Florida, 2006.
- [15] A.J.W. Johnson, K.S. Kumar, C.L. Briant, *Metall. Mater. Trans. A* 34 (2003) 1869–1877.
- [16] S.C. Tjong, Y.W. Mai, *Compos. Sci. Technol.* 68 (2008) 583–601.
- [17] L. Geng, D.R. Ni, J. Zhang, Z.Z. Zheng, *J. Alloy Compd.* 463 (2008) 488–492.
- [18] S.L. Kampe, P. Sadler, L. Christodoulou, D.E. Larsen, *Metall. Mater. Trans. A* 25 (1994) 2181–2197.
- [19] B.A. Kolachev, A.A. Ilyin, V.A. Volodin, D.V. Ryndenkov, in: I.V. Gorynin, S.S. Ushkov (Eds.), *Titanium'99: Science and Technology*, Proc 9th World Conf. on Titanium Science and Technology, vol. 1, Central Research Institute of Structural Materials, St. Petersburg, Russia, 2000, p. 53.
- [20] T. Christman, A. Needleman, S. Suresh, *Acta Metall.* 37 (1989) 3029.
- [21] T.W. Clyne, P.J. Withers, *An Introduction to Metal Matrix Composites*, Cambridge University Press, Cambridge, 1993.
- [22] N. Shi, B. Wilnere, R.J. Arsenault, *Acta Metall.* 40 (1992) 2841–2854.
- [23] Z. Wang, T.-K. Chen, D.J. Lloyd, *Metall. Trans.* 24A (1993) 197.
- [24] V.C. Nardone, K.M. Prewo, *Scripta Metall.* 26 (1986) 43–48.
- [25] V.C. Nardone, *Scripta Metall.* 21 (1987) 1313–1318.
- [26] A.M.S. Antonio, F.S. Sanos, R.S. Strohaecker, *Compos. Sci. Technol.* 65 (2005) 1749–1755.